Available online at www.sciencedirect.com
ScienceDirect
Journal of Magnetism and Magnetic Materials 320 (2008) 2079–2082
www.elsevier.com/locate/jmmm

Magnetic properties, microstructure, and phase evolution of $Pr_xFe_{bal.}Ti_yB_{20-x}$ ($x = 4$–9; $y = 2.5$–5) nanocomposites

C.H. Chiu[a], H.W. Chang[a,b,*], C.W. Chang[a], W.C. Chang[a,**]

[a]Department of Physics, National Chung Cheng University, Taiwan, ROC
[b]Institute of Physics, Academia Sinica, NanKang, Taipei, Taiwan, ROC

Received 22 November 2006
Available online 25 March 2008

Abstract

Magnetic properties, microstructure, and phase evolution of Pr lean and boron-enriched $Pr_xFe_{bal.}Ti_yB_{20-x}$ ($x = 4$–9; $y = 2.5$–5) melt-spinning ribbons with nanostructures have been investigated. Based on thermal magnetic analysis (TMA), for $y = 2.5$, two phases, namely $Pr_2Fe_{14}B$ and α-Fe, were found for ribbons with $x = 9$, while additional two metastable phases, $Pr_2Fe_{23}B_3$ and Fe_3B, existed for $x = 4$, 7 and 8. With the decrease of Pr content, the remanence increases but coercivity decreases. The optimal properties of $B_r = 9.5$ kG, ${}_iH_c = 10.7$ kOe, and $(BH)_{max} = 17.8$ MG Oe are achieved in $Pr_9Fe_{bal.}Ti_{2.5}B_{11}$ nanocomposites. On the other hand, higher Ti substitution for Fe in $Pr_7Fe_{bal.}Ti_yB_{13}$ ribbons could refine the grain size and suppress the metastable $Pr_2Fe_{23}B_3$ and Fe_3B phases effectively. The excellent permanent magnetic properties are mainly dominated by the nanoscaled microstructures and the coexistence of sufficient magnetically soft phases, Fe_3B, $Pr_2Fe_{23}B_3$ and α-Fe, with magnetically hard $Pr_2Fe_{14}B$ phase.

PACS: 75.50.Kj; 75.50.Ww; 75.50.Bb

Keywords: Nanocomposite; Metastable phase; PrFeB; Magnetic property

1. Introduction

Two different types of nanocomposite ribbons, including $Nd_2Fe_{14}B$/α-Fe [1,2] and $Nd_2Fe_{14}B/Fe_3B$ [3,4], have been extensively developed via melt spinning in order to enhance the magnetic properties of ribbons. For the former nanocomposites, the boron concentration is normally as low as 5.5–7 at%, while it is extremely high, $B = 16$–20 at%, for the latter nanocomposites. However, very few studies have done to investigate magnetic properties, phase evolution, and microstructure of PrFeB-type nanocomposite ribbons in the phase transformation between α-$Fe/Pr_2Fe_{14}B$ and $Fe_3B/Pr_2Fe_{14}B$ region.

In our previous studies, B_r, ${}_iH_c$, and $(BH)_{max}$ values of 8.4–9.6 kG, 9.5–14.3 kOe, and $(BH)_{max}$ of 13.4–16.2 MG Oe, respectively, have been obtained on the ternary $Pr_{9.5-11.76}Fe_{bal.}B_{10}$ ribbons [5]. The ${}_iH_c$ reduces while retaining high B_r and $(BH)_{max}$ values in this composition region (boron of approximately 10 at%), as decreasing the rare-earth content from 11 to 8 at%. We attempted to increase the volume fraction of the soft phase and refine the average grain sizes in order to strengthen the exchange-coupling effect between the magnetically soft and hard grains. Unfortunately, when the rare-earth content is less than 9 at%, a large amount of $R_2Fe_{23}B_3$ phase appears. It leads to the reduction of the volume fraction of $R_2Fe_{14}B$ and the deterioration of the magnetic properties [5]. Similar result has been reported by Chen et al. in $Pr_9Fe_{91-z}B_z$ nanocomposites with $z = 8$–12 [6], that the optimum magnetic properties of $B_r = 8.7$ kG, ${}_iH_c = 6.3$ kOe and $(BH)_{max} = 12.4$ MG Oe merely were obtained in ternary $Pr_9Fe_{83}B_8$ ribbons. Nevertheless, our recent research [7,8]

*Corresponding author at: Department of Physics, National Chung Cheng University, Taiwan, ROC. Tel./fax: +886 5 2721091.
**Also corresponding author.
E-mail addresses: wei0208@gmail.com (H.W. Chang), phywcc@ccu.edu.tw (W.C. Chang).

0304-8853/$ - see front matter © 2008 Elsevier B.V. All rights reserved.
doi:10.1016/j.jmmm.2008.03.026

has shown that a slight substitution of Ti for Fe in nearby $Pr_2Fe_{23}B_3$ ($Pr_{7.14}Fe_{82.14}B_{10.72}$) compositions is effective in suppressing the formation of metastable $Pr_2Fe_{23}B_3$ phase, which results in the presence of large amount of $Pr_2Fe_{14}B$ and α-Fe phases of fine grain sizes in the matrix even at lower annealing temperature. In Fe–B/$Nd_2Fe_{14}B$-type of Hirosawa's study [9], the magnetic properties of $B_r = 8.9$ kG, ${}_iH_c = 7.8$ kOe and $(BH)_{max} = 15$ MG Oe also were obtained in TiC co-substituted $Nd_7Fe_{bal.}Ti_4B_{12}C_1$ ribbons. Based on the above previous experiences, in this paper, we are interested in adopting Ti containing ingots with the composition of $Pr_xFe_{bal.}Ti_yB_{20-x}$ ($x = 4$–9; $y = 2.5$–5), to prepare melt-spun ribbons, attempting to investigate the variation of magnetic properties, phases, and microstructures.

2. Experiment

Alloy ingots with nominal compositions of $Pr_xFe_{bal.}Ti_yB_{20-x}$ ($x = 4$, 7, 8, and 9; $y = 2.5$, 4, or 5) were prepared by vacuum induction melting. Melt-spun ribbons were produced from ingots with wheel speeds ranging from 10 to 30 m/s. The ribbons selected were annealed at 600–700 °C for 10 min to optimize crystallization and to improve the permanent magnetic properties. Magnetic phases were determined by a Perkin-Elmer (model: TGA7) thermal gravimetric analyzer (TGA) with an externally applied magnetic field of 100 Oe (conventionally referred to as "TMA"). The magnetic properties, temperature coefficients and Henkel Plot [10,11] of the ribbons were measured by a DMS (model: 7035B) vibrating sample magnetometer (VSM). All samples were magnetized by a 40 kOe peak pulse field prior to the VSM measurement. The microstructures of ribbons are directly observed by a JEOL 100CX2 transmission electron microscopy (TEM).

3. Results and discussion

Table 1 lists B_r, ${}_iH_c$, and $(BH)_{max}$ values of melt-spun $Pr_xFe_{bal.}Ti_yB_{20-x}$ ($x = 4$–9; $y = 2.5$, 4, or 5) ribbons which follows their optimal crystallization treatment, along with the temperature coefficients of induction (commonly referred to as α for B_r and β for ${}_iH_c$) for the temperature range of 25–100 °C. For the ribbons with $y = 2.5$, it can be found that B_r increases, but ${}_iH_c$ decreases monotonously with decreasing Pr content x. Besides, the $(BH)_{max}$ value sharply decreases from 17.8 to 8.3 MG Oe when x is decreased from 9 to 4. Among all ribbons, the optimal magnetic properties of $B_r = 9.5$ kG, ${}_iH_c = 10.7$ kOe, and $(BH)_{max} = 17.8$ MG Oe are obtained in $Pr_9Fe_{bal.}Ti_{2.5}B_{11}$.

Table 1
B_r, ${}_iH_c$, and $(BH)_{max}$ values of melt-spun $Pr_xFe_{bal.}Ti_yB_{20-x}$ ($x = 4$ to 9; $y = 2.5$, 4, or 5) ribbons following their optimal crystallization treatment, along with the temperature coefficients of induction (commonly referred to as α for B_r and β for ${}_iH_c$) for the temperature range of 25–100 °C

x	y	B_r (kG)	${}_iH_c$ (koe)	$(BH)_{max}$ (MgOe)	α (%/°C)	β (%/°C)
					25–100 °C	
9	2.5	9.5	10.7	17.8	−0.135	−0.576
8	2.5	9.6	8.1	16.2	−0.136	−0.580
7	2.5	9.7	5.5	10.8	−0.143	−0.588
4	2.5	10.2	3.5	8.3	−0.155	−0.618
7	4	9.0	7.8	13.3	−0.139	−0.585
7	5	9.2	9.6	15.8	−0.136	−0.579

On the other hand, the ${}_iH_c$ and $(BH)_{max}$ can be enhanced from 5.5 and 10.8 to 7.8 kOe and 13.3 MG Oe, respectively, with increasing Ti content from $y = 2.5$ to $y = 4$ in the $Pr_7Fe_{bal.}Ti_yB_{13}$ series ribbons. In addition, as Ti content is increased to $y = 5$ in the $Pr_7Fe_{bal.}Ti_5B_{13}$ ribbon, the magnetic properties can be further enhanced to 9.6 kOe and 15.8 MG Oe. For temperature coefficients, the value of α and β of $Pr_xFe_{bal.}Ti_{2.5}B_{20-x}$ increases with decreasing x, which reflects that decreasing Pr content in the studied alloys degrades the thermal stability of ribbons. On the contrary, more Ti ($y = 4$ or 5) substitution for Fe in the $Pr_7Fe_{76}Ti_yB_{13}$ ribbon can decrease the value of α and β to enhance the thermal stability of ribbons.

Fig. 1 presents TMA scans of melt-spun $Pr_xFe_{bal.}Ti_yB_{20-x}$ ribbons with optimal annealing treatment. For $y = 2.5$ series nanocomposite ribbons, it is found that ribbons with $x = 9$ have only two magnetic phases, hard magnetic phase $Pr_2Fe_{14}B$ and soft magnetic phase α-Fe. However, four phases, including $Pr_2Fe_{14}B$, α-Fe, metastable

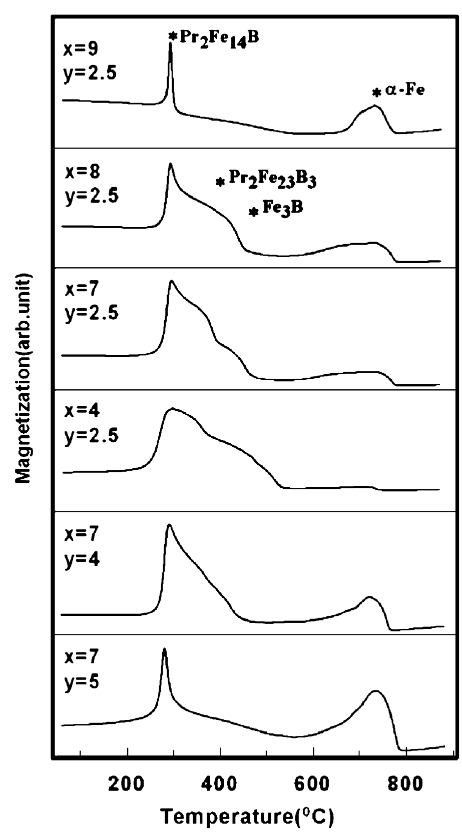

Fig. 1. TMA scans of melt-spun $Pr_xFe_{bal.}Ti_yB_{20-x}$ ribbons with optimal annealing treatment.